Electronic Supplementary Material (ESI) for CrystEngComm.
This journal is © The Royal Society of Chemistry 2024

Electronic Supplementary Information (ESI)

Co-crystal Formation vs. Boron Coordination: Fluorination in Azopyridines Regulates Supramolecular Competition

Jesus Daniel Loya,[a,†] Sidhaesh A. Agarwal,[a,†] Nicholas Lutz,[a] Eric W. Reinheimer,[b] and Gonzalo Campillo-Alvarado[a,*]

[a]Department of Chemistry, Reed College, Portland, OR 97202, USA.
[b]Rigaku Oxford Diffraction, The Woodlands, Texas, 77381, USA
[†]These authors contributed equally.

*e-mail: gcampillo@reed.edu

Table of Contents:

S1. Experimental information

Materials:
3-Fluoro-4-aminopyridine, 3,5-difluoro-4-aminopyridine, 2,3,5,6-tetrafluoro-4-aminopyridine, 4,4'-azopyiridine, phenylboronic acid were obtained from AmBeed. Catechol was purchased from TCI. Acetonitrile, dichloromethane (DCM), deuterated water (DI), $MgSO_4$, and sodium hypochlorite solution were obtained from Sigma-Aldrich. All reagents and solvent were used as received.

General synthetic method of azopyridines:
The synthetic procedure was adapted from the literature.[1] A fluorinated aminopyridine (500 mg) was dissolved in DI water (100 mL) to which 40 mL cold sodium hypochlorite solution was added dropwise with vigorous stirring at 0˚C affording a deep yellow solution. The aqueous layer was extracted with DCM (3 x 100 mL). The resulting solution was dried over $MgSO_4$ and filtered. The filtrate was concentrated to produce crystalline solids.

Synthesis of **diF-azop**: 3-fluoro-4-aminopyridine was reacted using the general synthetic method of azopyridines to afford **diF-azop** as a red solid. Recrystallization in acetonitrile afforded single crystals as black planks (210.3 mg, 42.8 %). ^{1}H NMR (400 MHz, $CDCl_3$) δ 8.80 (d, *J* = 2.0 Hz, 2H), 8.61 (d, *J* = 5.0 Hz, 2H), 7.59 (t, *J* = 5.7 Hz, 2H) ppm; ^{19}F NMR (376 MHz, $CDCl_3$) δ -138 (s, 2F) ppm; ^{19}F NMR spectrum showed traces the of *cis* isomer.

Synthesis of **tetraF-azop**: 3,5-difluoro-4-aminopyridine was reacted using the general synthetic method of azopyridines to afford **tetraF-azop** as a red solid. Recrystallization in acetonitrile afforded single crystals in the form of black blocks (279.80 mg, 56.8 %). ^{1}H NMR (400 MHz, $CDCl_3$) δ 8.54 (m, 4H) ppm; ^{19}F NMR (376 MHz, $CDCl_3$) δ -137 (s, 4F) ppm. ^{19}F NMR showed the presence of *cis*:*trans* isomers (ratio: 17:83).

Synthesis of **perF-azop**: 2,3,5,6-tetrafluoro-4-aminopyridine was reacted using an adapted procedure using 500 mL of DI water rather than 100 mL. **perf-azop** was isolated as a red solid. Single crystals in the form of red irregular planks were obtained after rotary evaporation (140.00 mg, 28.3%). ^{19}F NMR (376 MHz, $CDCl_3$) δ -87 (m, 2F), -150 (m, 2F) ppm. Note: ^{19}F NMR showed the presence of *cis*:*trans* isomers (ratio: 17:83).

General synthetic method of adducts
Azopyridine (**azop**, **diF-azop**, **tetraF-azop**) (0.015 mmol) was combined with phenylboronic acid (**PhBA**, 0.30 mmol) and catechol (**cat**, 0.30 mmol) in acetonitrile (3 mL). The solutions were gently heated until the solids fully dissolved. Single crystals of the adducts (**PhBE**)·(**diF-azop**), (**PhBE**)·(**tetraF-azop**) were observed after three days of

slow evaporation. For the case of (**PhBE**)·(**azop**), the vial containing the solution was sealed, and single crystals were observed after three days under 4 °C.

Synthesis of (**PhBE**)·(**perF-azop**): **perF-azop** (0.015 mmol) was combined with **PhBA** (0.15 mmol) and **cat**, (0.15 mmol) in acetonitrile (3 mL). The solution was gently heated until the solids fully dissolved. Single crystals of (**PhBE**)·(**perF-azop**) were observed after three days of slow evaporation. Initial attempts using **perF-azop** (0.015 mmol) with **PhBA** (0.30 mmol) and **cat** (0.30 mmol) afforded crystals of (**PhBE**)·(**perF-azop**) with the presence of crystal of pure **PhBE**.

We note adducts (**PhBE**)·(**azop**), (**PhBE**)·(**diF-azop**), and (**PhBE**)·(**tetraF-azop**) hydrolyze when dissolved in DMSO-d_6 into the corresponding azopyridine, catechol and phenylboronic acid

All the synthesized solids were protected from light in vials wrapped with aluminum foil. X-ray diffraction experiments were performed in an environment with minimum light.

Instruments and methods:

^{1}H and ^{19}F NMR spectra were recorded on a Bruker Ascend Evo 400 MHz spectrometer with chloroform-d, DMSO-d_6 and TMS as internal standards. ^{19}F NMR experiments were decoupled. NMR data was processed with Mnova suite. Single crystal X-ray diffraction (SCXRD) data was collected on a Rigaku XtaLAB Mini II diffractometer with a CCD area detector (λMoKα = 0.71073 Å, monochromator: graphite). Experiments were conducted at 100 K with a range of 2θ = 3-62°. The collected data was refined with CrysAlisPro through standard data reduction and background corrections (multi-scan was used for all samples). Crystals were mounted in Paratone oil on a Mitegen magnetic mount. Structure solution and refinement were performed using SHELXT[2] and SHELXL,[3] respectively within the Olex2[4] graphical user interface. All the hydrogen atoms were added in geometrically calculated positions using a riding model with appropriate AFIX instructions.

Computational methods:

Single point energy calculations at ground state in the gas phase were performed using the Spartan ’20 graphical user interface using geometrical coordinates obtained from single crystal X-ray diffraction data. Density Functional Theory (DFT) was used with the ωB97X-D exchange-correlation functional and correlated corrected basis set cc-pVTZ.[5] Electrostatic potential maps were computed and mapped using the isodensity surface 0.002 e/au^3 with medium resolution.

S2. Single-crystal X-ray data

Table S1. Crystallographic parameters for (**PhBE**)·(**azop**)

Compound name	(**PhBE**)·(**azop**)
Empirical formula	$C_{34}H_{26}B_2N_4O_4$
Formula weight	576.21
Temperature/K	99.9(6)
Crystal system	monoclinic
Space group	$P2_1/c$
a/Å	6.8631(2)
b/Å	13.1490(3)
c/Å	15.7054(4)
α/°	90
β/°	99.615(3)
γ/°	90
Volume/Å^3	1397.39(6)
Z	2
ρ_{calc}g/cm^3	1.369
μ/mm^{-1}	0.090
F(000)	600.0
Crystal size/mm^3	0.32 × 0.25 × 0.17
Radiation	Mo Kα (λ = 0.71073)
2Θ range for data collection/°	4.064 to 61.294
Index ranges	-9 ≤ h ≤ 9, -17 ≤ k ≤ 18, -22 ≤ l ≤ 20
Reflections collected	12564
Independent reflections	4129 [R_{int} = 0.0275, R_{sigma} = 0.0320]
Data/restraints/parameters	4129/15/222
Goodness-of-fit on F^2	1.039
Final R indexes [I>=2σ (I)]	R_1 = 0.0543, wR_2 = 0.1366
Final R indexes [all data]	R_1 = 0.0669, wR_2 = 0.1442
CCDC deposition number	2347089

Table S2. Crystallographic parameters for (**PhBE**)·(**diF-azop**)

Compound name	(**PhBE**)·(**diF-azop**)
Empirical formula	$C_{34}H_{24}B_2F_2N_4O_4$
Formula weight	612.19
Temperature/K	99.9(6)
Crystal system	monoclinic
Space group	$P2_1/c$
a/Å	6.8710(3)
b/Å	13.0541(6)
c/Å	15.9373(7)
α/°	90
β/°	97.627(4)
γ/°	90
Volume/Å^3	1416.86(11)
Z	2
ρ_{calc}g/cm^3	1.435
μ/mm^{-1}	0.103
F(000)	632.0
Crystal size/mm^3	0.47 × 0.24 × 0.11
Radiation	Mo Kα (λ = 0.71073)
2Θ range for data collection/°	4.048 to 49.996
Index ranges	$-8 \le h \le 8$, $-15 \le k \le 15$, $-14 \le l \le 18$
Reflections collected	9101
Independent reflections	2494 [R_{int} = 0.0788, R_{sigma} = 0.0636]
Data/restraints/parameters	2494/0/208
Goodness-of-fit on F^2	1.049
Final R indexes [I>=2σ (I)]	R_1 = 0.0508, wR_2 = 0.1356
Final R indexes [all data]	R_1 = 0.0637, wR_2 = 0.1436
CCDC deposition number	2347091

Table S3. Crystallographic parameters for (**PhBE**)·(**tetraF-azop**)

Compound name	**(PhBE)·(tetraF-azop)**
Empirical formula	$C_{34}H_{22}B_2F_4N_4O_4$
Formula weight	648.17
Temperature/K	100.00(6)
Crystal system	monoclinic
Space group	$P2_1/c$
a/Å	7.0434(4)
b/Å	12.8068(7)
c/Å	16.0013(9)
α/°	90
β/°	98.123(5)
γ/°	90
Volume/Å^3	1428.89(14)
Z	2
ρ_{calc}g/cm^3	1.507
μ/mm^{-1}	0.117
F(000)	664.0
Crystal size/mm^3	0.19 × 0.13 × 0.09
Radiation	Mo Kα (λ = 0.71073)
2Θ range for data collection/°	4.09 to 49.992
Index ranges	$-8 \le h \le 8$, $-15 \le k \le 15$, $-19 \le l \le 19$
Reflections collected	9008
Independent reflections	2526 [R_{int} = 0.0747, R_{sigma} = 0.0815]
Data/restraints/parameters	2526/0/217
Goodness-of-fit on F^2	0.978
Final R indexes [I>=2σ (I)]	R_1 = 0.0446, wR_2 = 0.0997
Final R indexes [all data]	R_1 = 0.0755, wR_2 = 0.1104
CDCC deposition number	2347088

Table S4. Crystallographic parameters for (**PhBE**)·(**perF-azop**)

Compound name	**(PhBE)·(perF-azop)**
Empirical formula	$C_{22}H_9BF_8N_4O_2$
Formula weight	524.14
Temperature/K	99.9(5)
Crystal system	triclininc
Space group	*P*-1
a/Å	6.2144(12)
b/Å	7.2948(13)
c/Å	11.7785(17)
α/°	81.392(13)
β/°	77.890(15)
γ/°	85.140(16)
Volume/Å^3	515.41(16)
Z	1
ρ_{calc}g/cm^3	1.689
μ/mm^{-1}	0.159
F(000)	262.0
Crystal size/mm^3	0.552 × 0.161 × 0.089
Radiation	Mo Kα (λ = 0.71073)
2Θ range for data collection/°	5.656 to 52.744
Index ranges	-7 ≤ h ≤ 7, -9 ≤ k ≤ 9, -14 ≤ l ≤ 14
Reflections collected	6510
Independent reflections	2083 [R_{int} = 0.0498, R_{sigma} = 0.0590]
Data/restraints/parameters	2083/90/208
Goodness-of-fit on F^2	1.013
Final R indexes [I>=2σ (I)]	R_1 = 0.0544, wR_2 = 0.1403
Final R indexes [all data]	R_1 = 0.0827, wR_2 = 0.1614
CCDC deposition number	2347087

Table S5. Crystallographic parameters for **diF-azop**

Compound name	**diF-azop**
Empirical formula	$C_{10}H_6F_2N_4$
Formula weight	220.19
Temperature/K	99.9(7)
Crystal system	orthorhombic
Space group	*Pbca*
a/Å	6.6796(6)
b/Å	12.6700(7)
c/Å	22.3037(14)
α/°	90
β/°	90
γ/°	90
Volume/Å^3	1887.6(2)
Z	8
ρ_{calc}g/cm^3	1.550
μ/mm^{-1}	0.127
F(000)	896.0
Crystal size/mm^3	0.267 × 0.072 × 0.063
Radiation	Mo Kα (λ = 0.71073)
2Θ range for data collection/°	6.432 to 49.984
Index ranges	-7 ≤ h ≤ 7, -14 ≤ k ≤ 13, -26 ≤ l ≤ 26
Reflections collected	13924
Independent reflections	1651 [R_{int} = 0.0927, R_{sigma} = 0.0674]
Data/restraints/parameters	1651/0/145
Goodness-of-fit on F^2	0.958
Final R indexes [I>=2σ (I)]	R_1 = 0.0568, wR_2 = 0.1419
Final R indexes [all data]	R_1 = 0.0850, wR_2 = 0.1557
CCDC deposition number	2347092

Table S6. Crystallographic parameters for **tetraF-azop**

Compound name	**tetraF-azop**
Empirical formula	$C_{10}H_4F_4N_4$
Formula weight	256.17
Temperature/K	99.9(7)
Crystal system	monoclinic
Space group	$P2_1/c$
a/Å	5.0686(6)
b/Å	5.1891(7)
c/Å	18.590(2)
α/°	90
β/°	90.109(12)
γ/°	90
Volume/Å^3	488.96(11)
Z	2
ρ_{calc}g/cm^3	1.740
μ/mm^{-1}	0.164
F(000)	256.0
Crystal size/mm^3	0.54 × 0.5 × 0.05
Radiation	Mo Kα (λ = 0.71073)
2Θ range for data collection/°	4.382 to 49.982
Index ranges	-6 ≤ h ≤ 5, -6 ≤ k ≤ 6, -21 ≤ l ≤ 22
Reflections collected	2309
Independent reflections	848 [R_{int} = 0.0390, R_{sigma} = 0.0542]
Data/restraints/parameters	848/0/83
Goodness-of-fit on F^2	1.107
Final R indexes [I>=2σ (I)]	R_1 = 0.0478, wR_2 = 0.1287
Final R indexes [all data]	R_1 = 0.0565, wR_2 = 0.1351
CCDC deposition number	2347090

Table S7. Crystallographic parameters for **perF-azop**

Compound name	**perF-azop**
Empirical formula	$C_{10}F_8N_4$
Formula weight	328.14
Temperature/K	100.15
Crystal system	monoclinic
Space group	$P2_1/c$
a/Å	5.8251(6)
b/Å	15.5339(18)
c/Å	5.9792(8)
α/°	90
β/°	100.851(12)
γ/°	90
Volume/Å^3	531.36(11)
Z	2
ρ_{calc}g/cm^3	2.051
μ/mm^{-1}	0.228
F(000)	320.0
Crystal size/mm^3	0.17 × 0.07 × 0.04
Radiation	Mo Kα (λ = 0.71073)
2Θ range for data collection/°	5.244 to 49.984
Index ranges	-6 ≤ h ≤ 6, -18 ≤ k ≤ 18, -7 ≤ l ≤ 7
Reflections collected	3070
Independent reflections	931 [R_{int} = 0.0596, R_{sigma} = 0.0889]
Data/restraints/parameters	931/0/100
Goodness-of-fit on F^2	1.031
Final R indexes [I>=2σ (I)]	R_1 = 0.0517, wR_2 = 0.1036
Final R indexes [all data]	R_1 = 0.0998, wR_2 = 0.1206
CCDC deposition number	2347086

S3. Powder X-ray Data and Phase Analysis

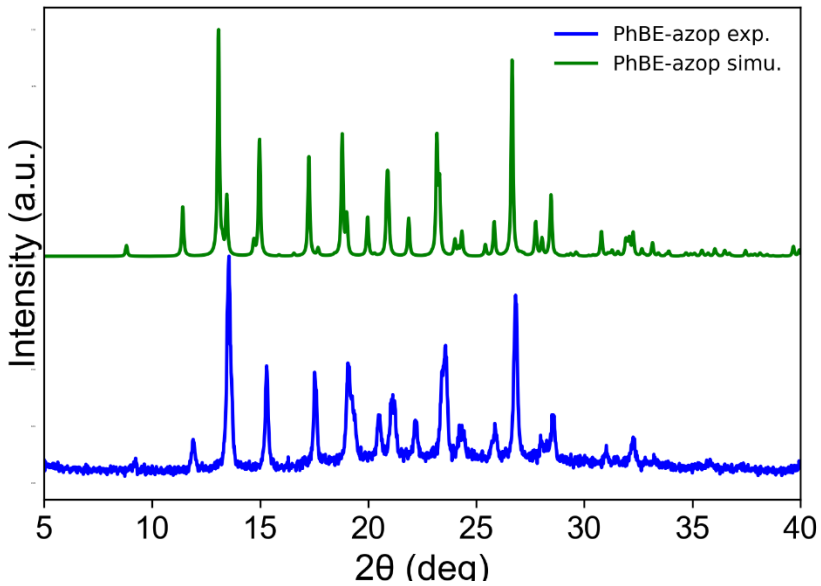

Figure S1. Powder X-ray diffractograms of (**PhBE**)·(**azop**) simulated from single crystal data (top) and experimental (bottom).

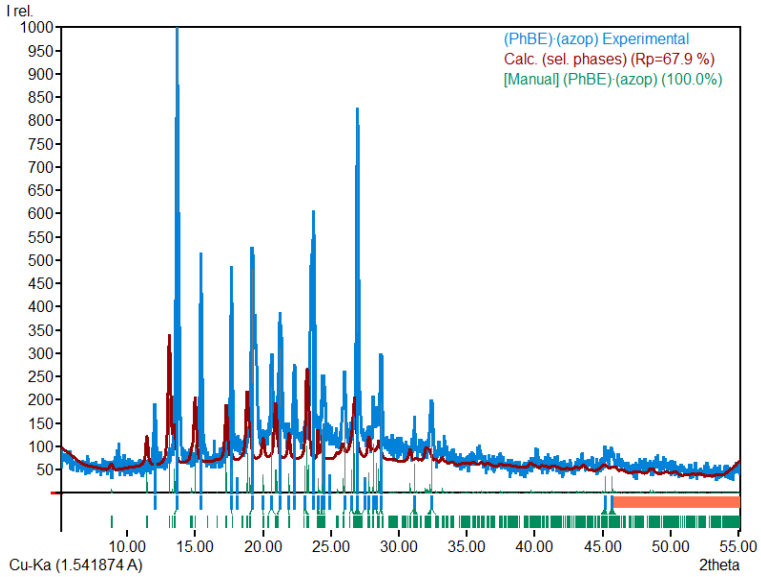

Figure S2. Phase composition analysis of (**PhBE**)·(**azop**) using experimental and simulated from single crystal data. Phase analysis was carried out using Match! software using profile fitting.[6]

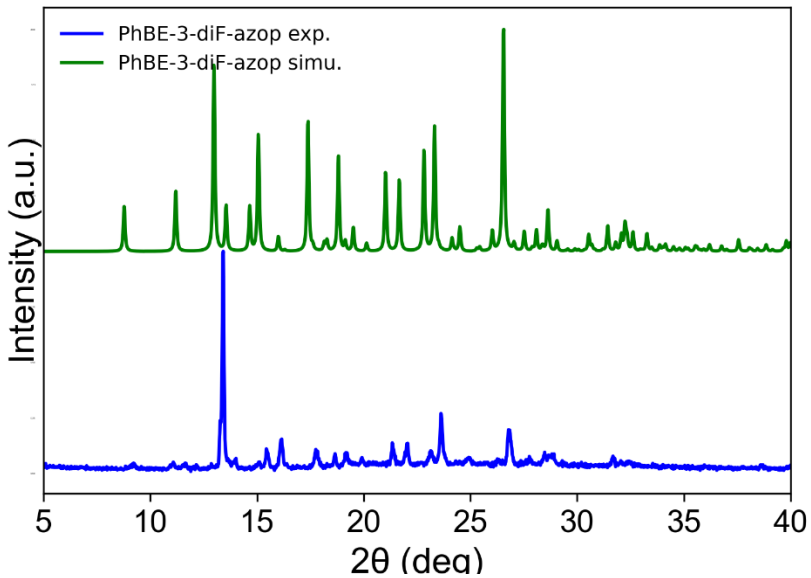

Figure S3. Powder X-ray diffractograms of (**PhBE**)·(**diF-azop**) simulated from single crystal data (top) and experimental (bottom).

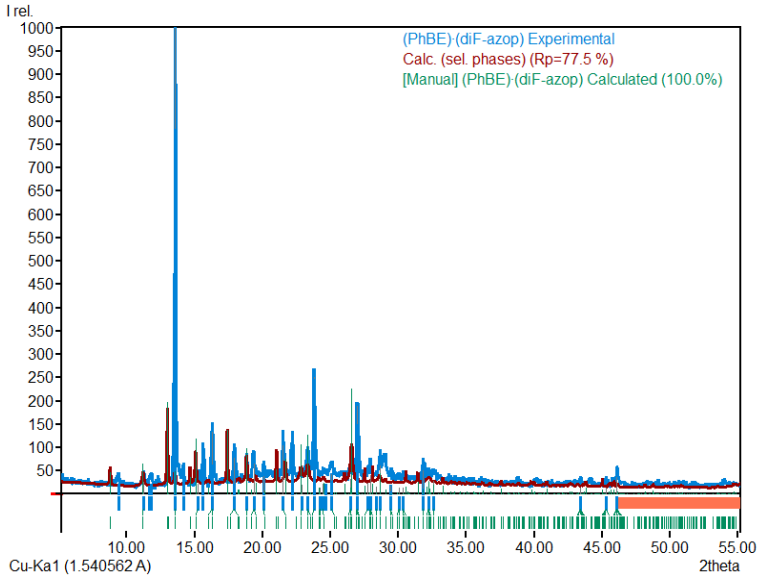

Figure S4. Phase composition analysis of (**PhBE**)·(**diFazop**) using experimental and simulated from single crystal data. Phase analysis was carried out using Match! software using profile fitting.[6]

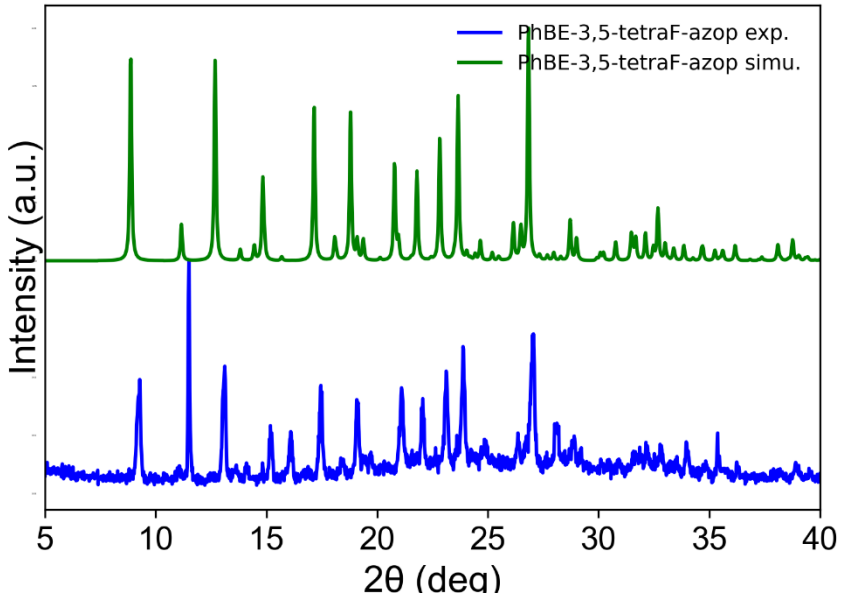

Figure S5. Powder X-ray diffractograms of (**PhBE**)·(**tetraF-azop**) simulated from single crystal data (top) and experimental (bottom).

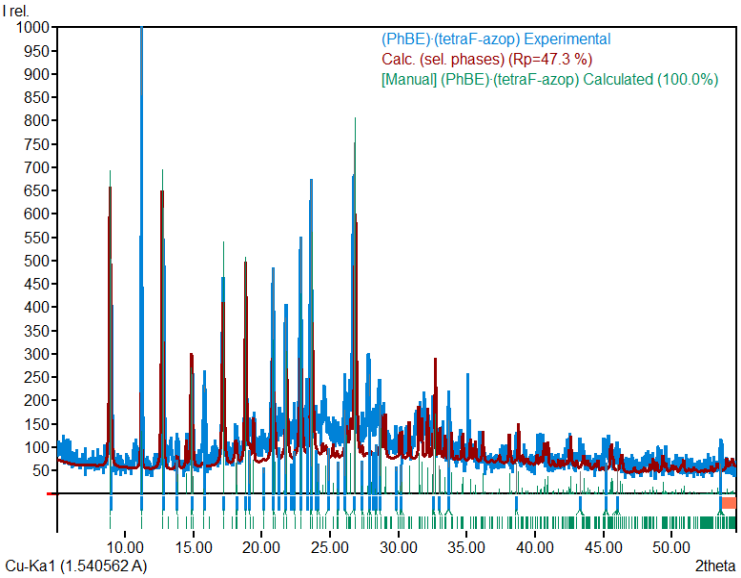

Figure S6. Phase composition analysis of (**PhBE**)·(**tetraFazop**) using experimental and simulated from single crystal data. Phase analysis was carried out using Match! software using profile fitting.[6]

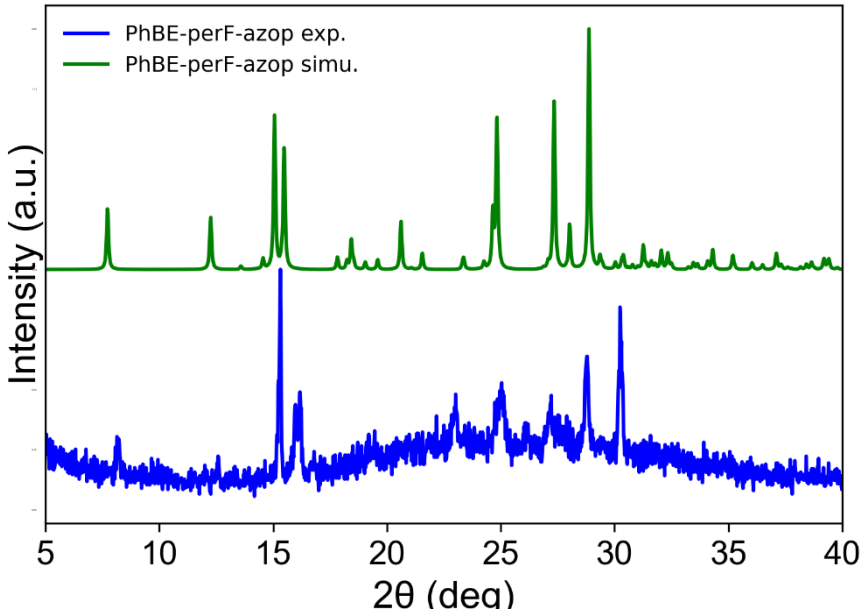

Figure S7. Powder X-ray diffractograms of (**PhBE**)·(**perF-azop**) simulated from single crystal data (top) and experimental (bottom).

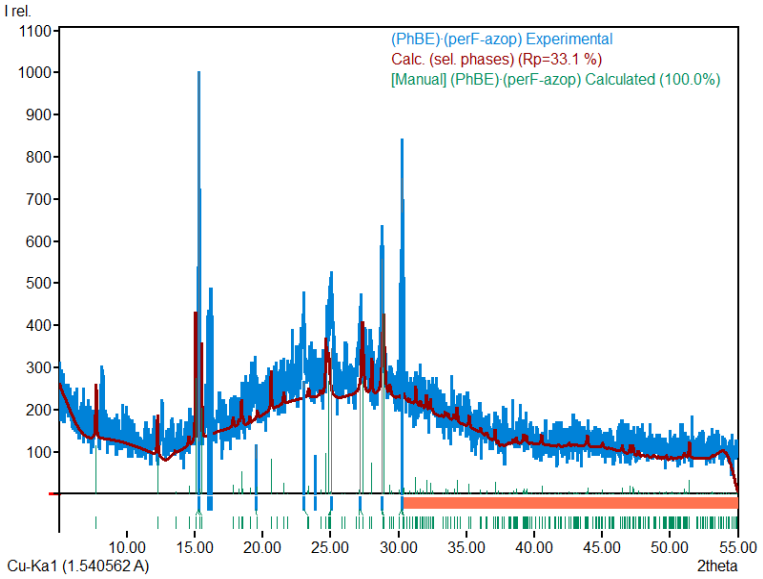

Figure S8. Phase composition analysis of (**PhBE**)·(**perFazop**) using experimental and simulated from single crystal data. Phase analysis was carried out using Match! software using profile fitting.[6]

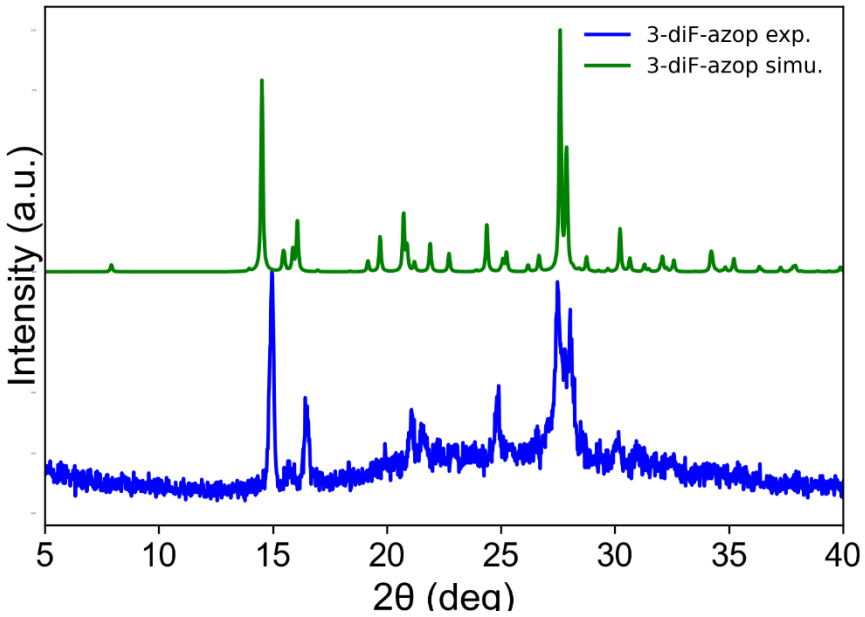

Figure S9. Powder X-ray diffractograms of **diF-azop** simulated from single crystal data (top) and experimental (bottom).

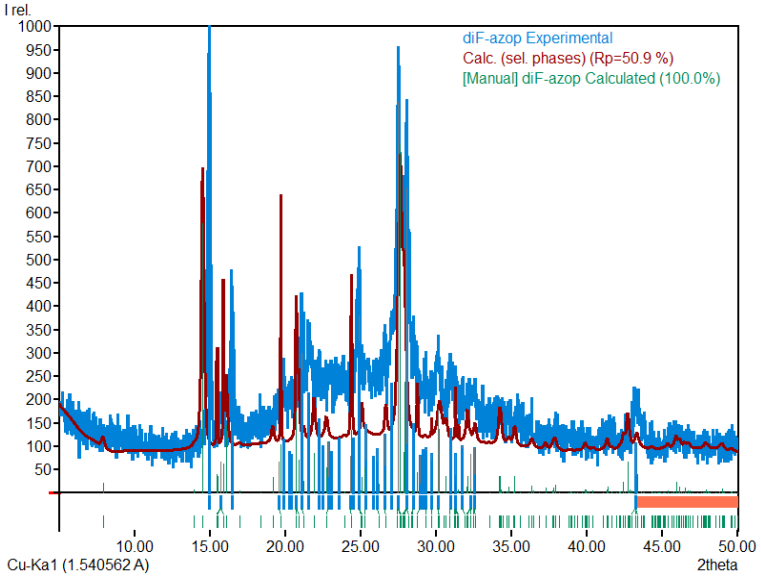

Figure S10. Phase composition analysis of **diFazop** using experimental and simulated from single crystal data. Phase analysis was carried out using Match! software using profile fitting.[6]

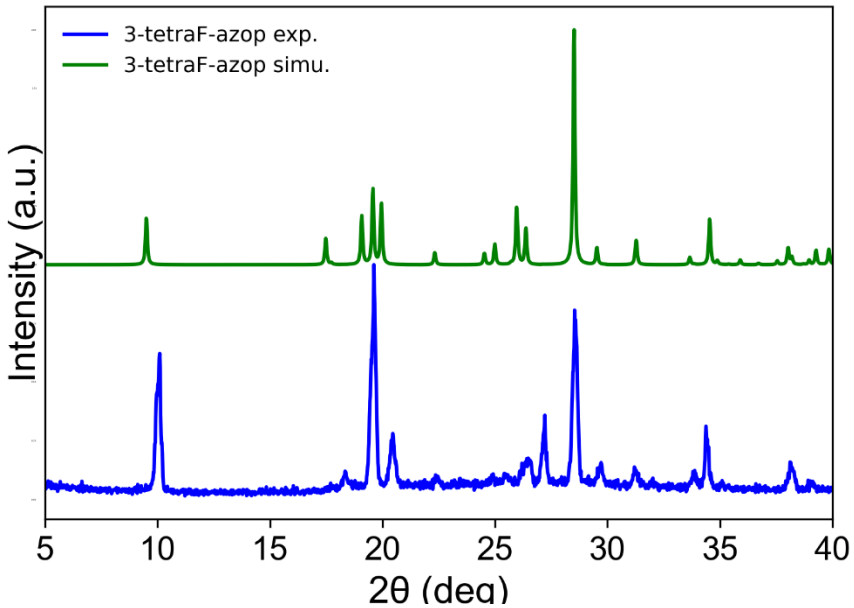

Figure S11. Powder X-ray diffractograms of **tetraF-azop** simulated from single crystal data (top) and experimental (bottom).

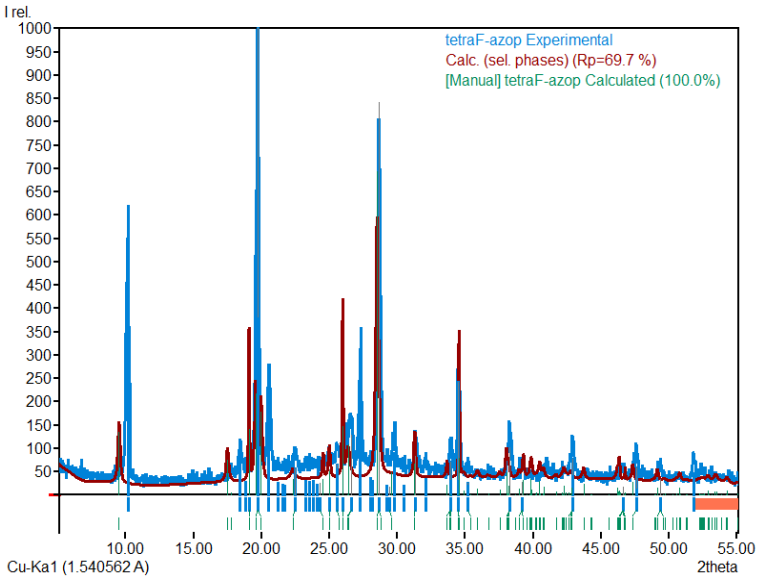

Figure S12. Phase composition analysis of **tetraFazop** using experimental and simulated from single crystal data. Phase analysis was carried out using Match! software using profile fitting.[6]

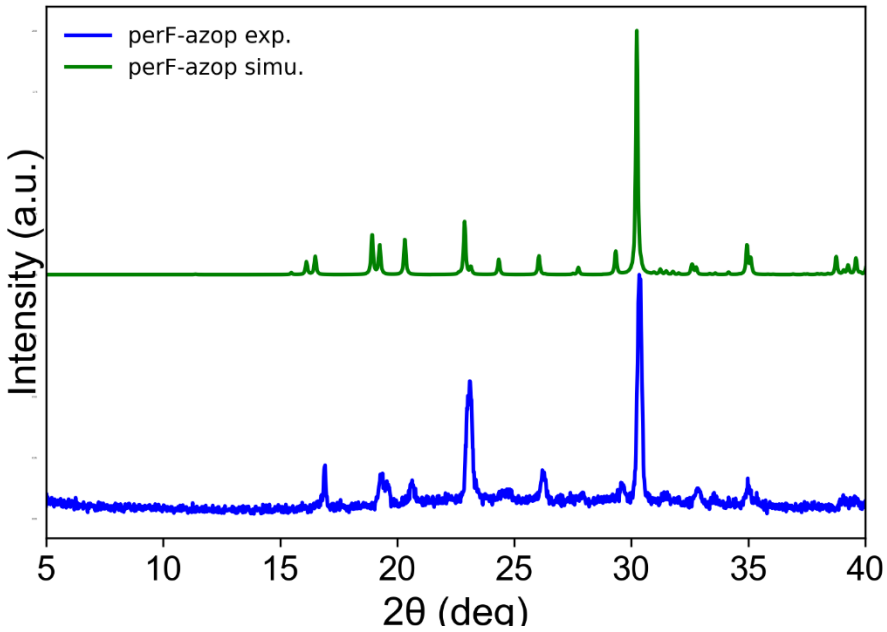

Figure S13. Powder X-ray diffractograms of **perF-azop** simulated from single crystal data (top) and experimental (bottom).

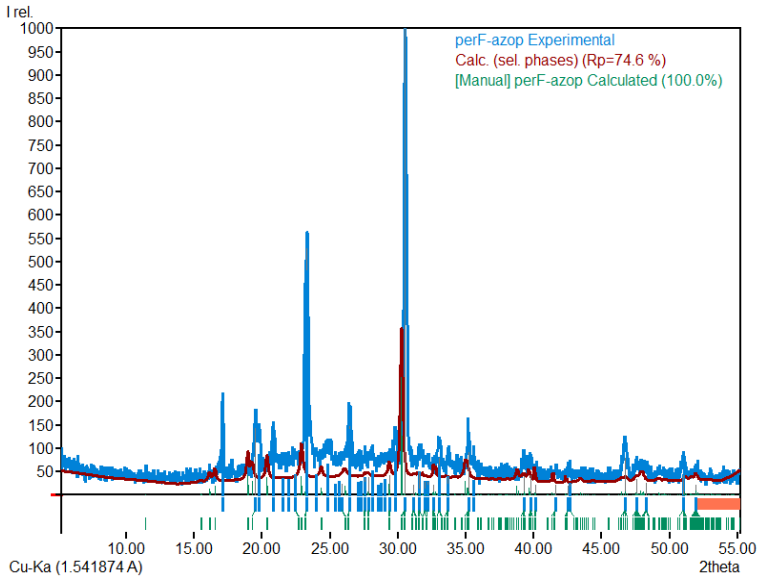

Figure S14. Phase composition analysis of **perF-azop** using experimental and simulated from single crystal data. Phase analysis was carried out using Match! software using profile fitting.[6]

S4. NMR Spectra

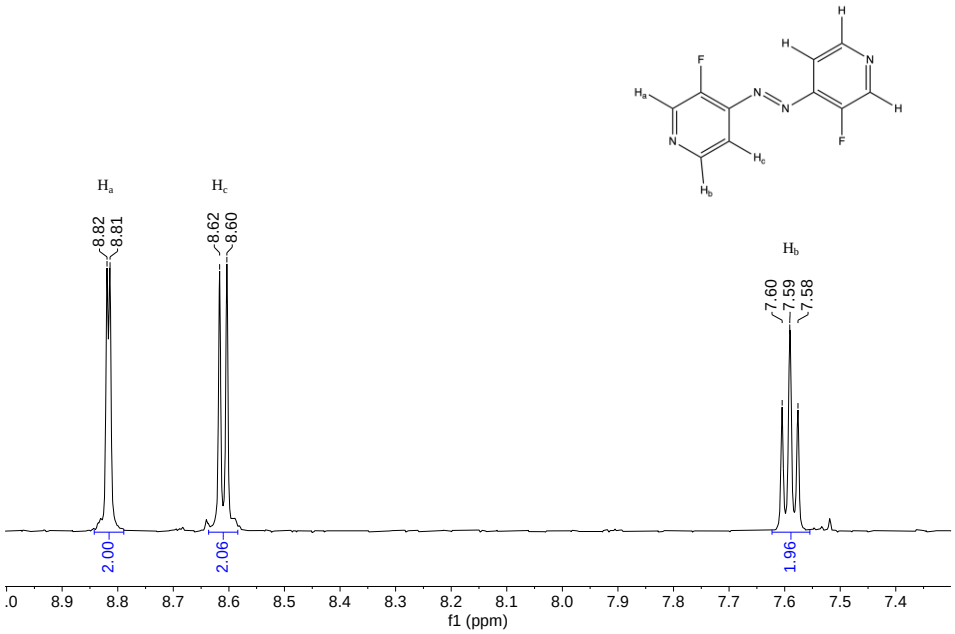

Figure S15. ^{1}H NMR spectra of **diF-azop** (400 MHz, $CDCl_3$).

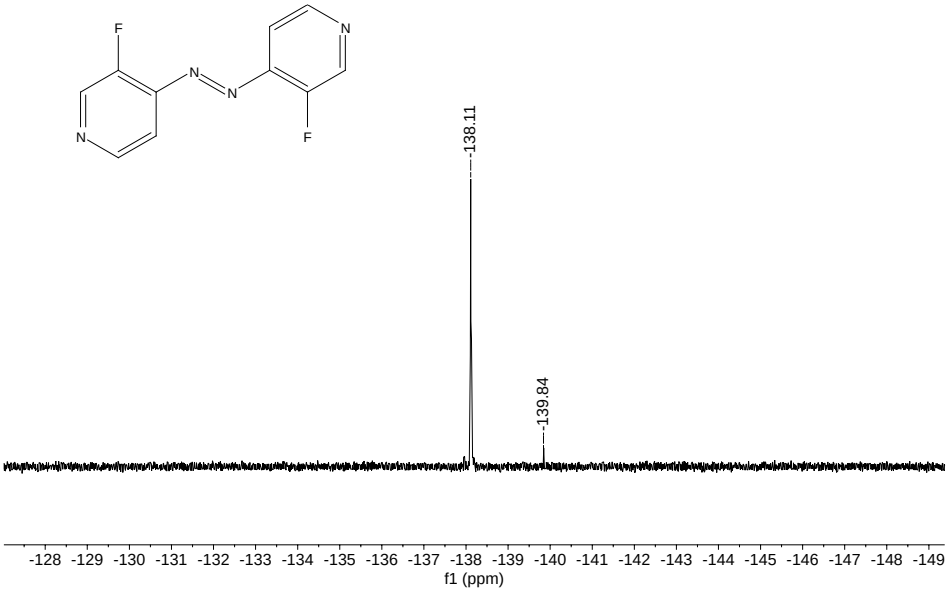

Figure S16. ^{19}F NMR spectra of **diF-azop** (400 MHz, $CDCl_3$).

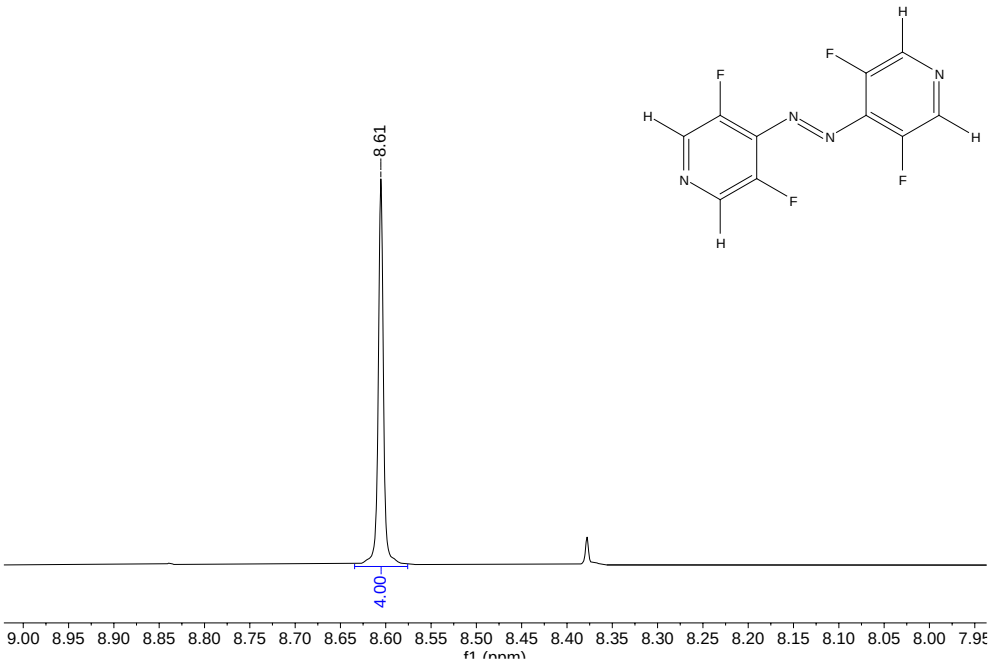

Figure S17. ^{1}H NMR spectra of **tetraF-azop** (400 MHz, $CDCl_3$).

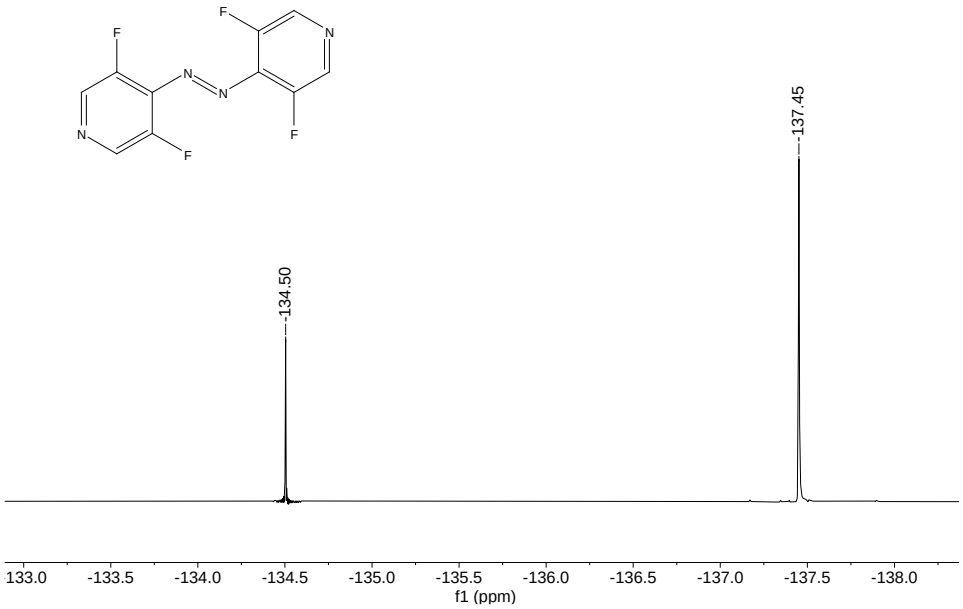

Figure S18. ^{19}F NMR spectra of **tetraF-azop** (400 MHz, $CDCl_3$).

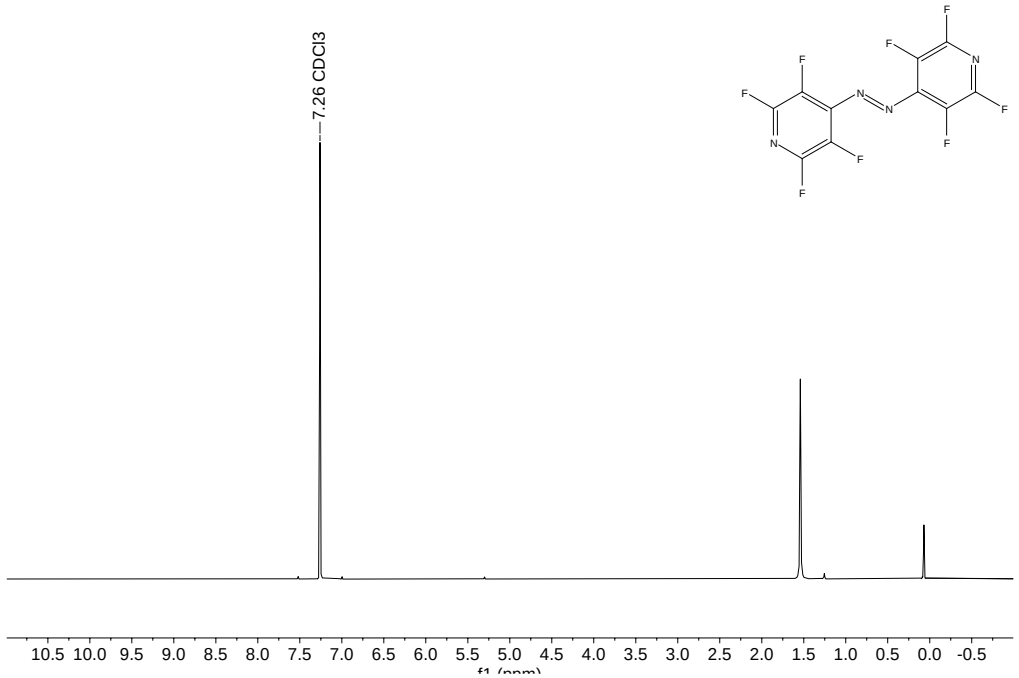

Figure S19. ^{1}H NMR spectra of **perF-azop** (400 MHz, $CDCl_3$).

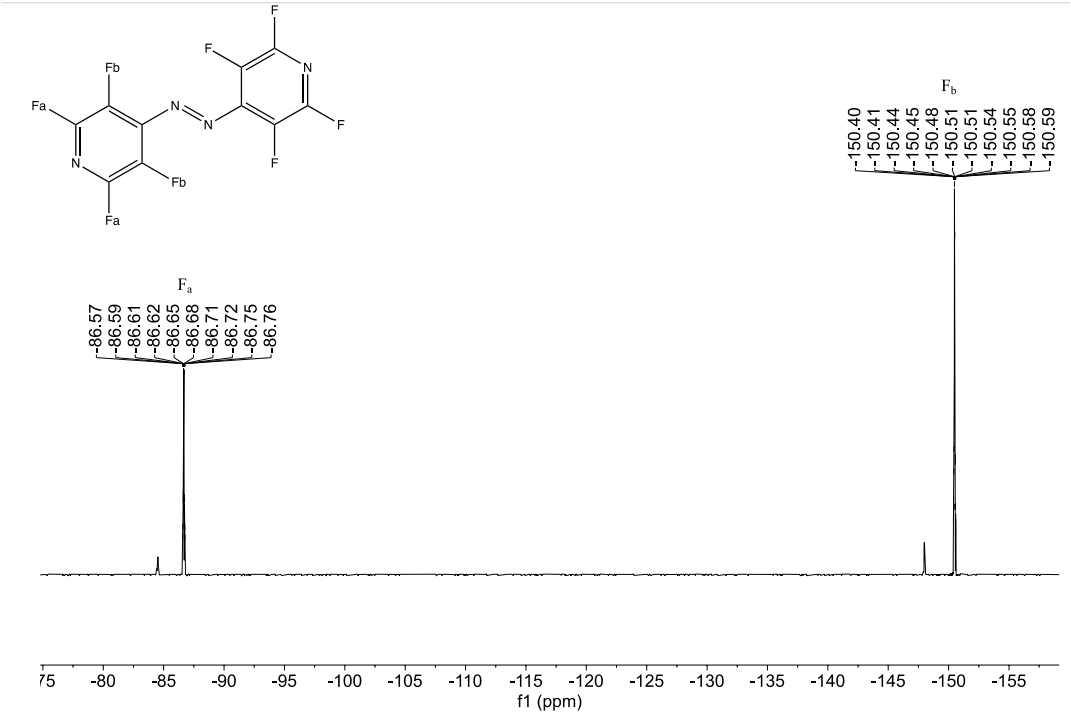

Figure S20. ^{19}F NMR spectra of **perF-azop** (400 MHz, $CDCl_3$).

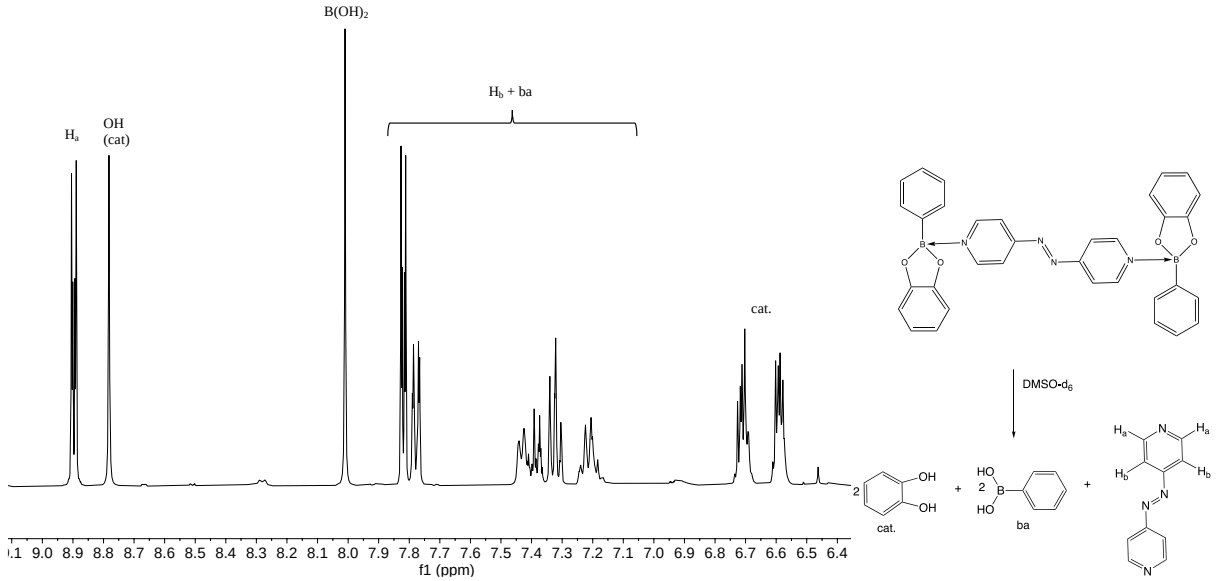

Figure S21. ^{1}H NMR spectra of (**PhBE**)·(**azop**) (400 MHz, DMSO-d_6). We note the adduct dissociated in solution.

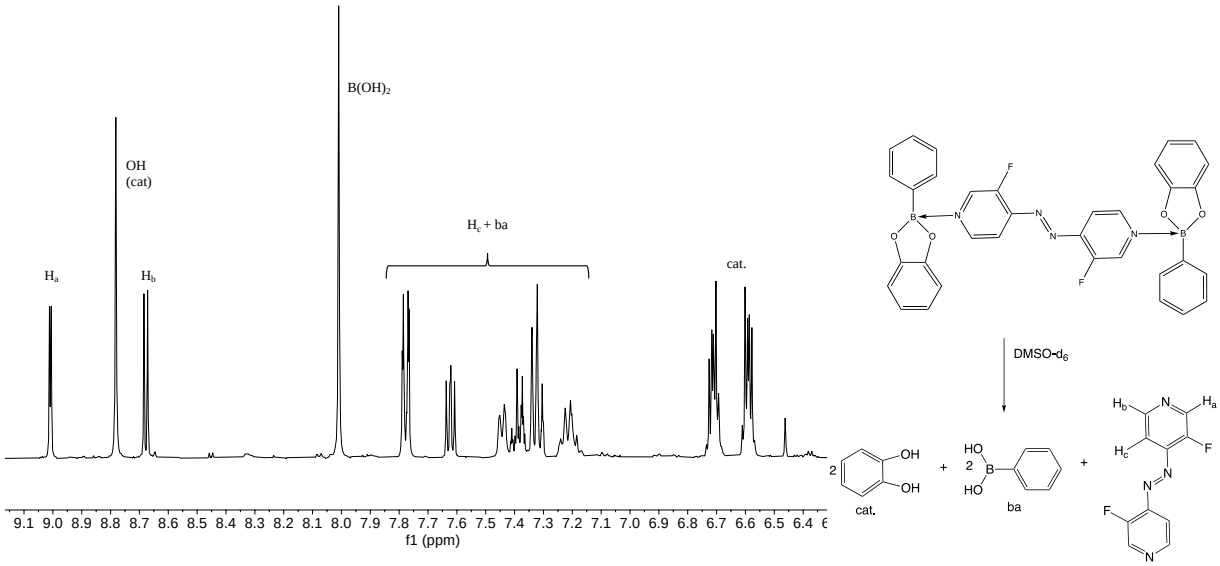

Figure S22. ^{1}H NMR spectra of (**PhBE**)·(**diF-azop**) (400 MHz, DMSO-d_6). We note the adduct dissociated in solution.

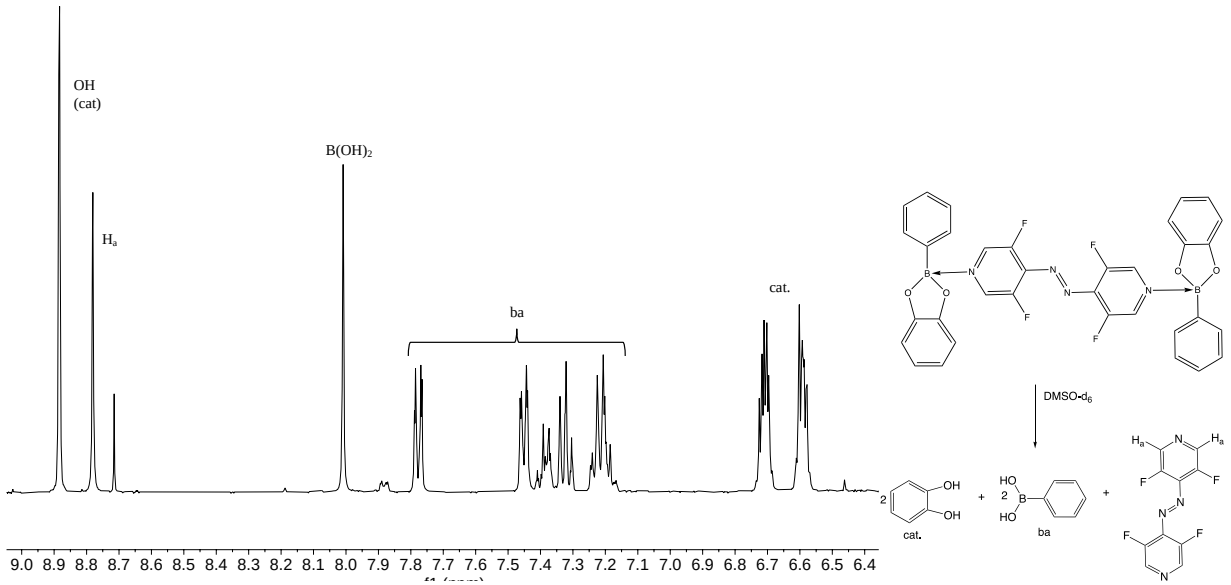

Figure S23. ^{1}H NMR spectra of (**PhBE**)·(**tetraF-azop**) (400 MHz, DMSO-d_6). We note the adduct dissociated in solution.

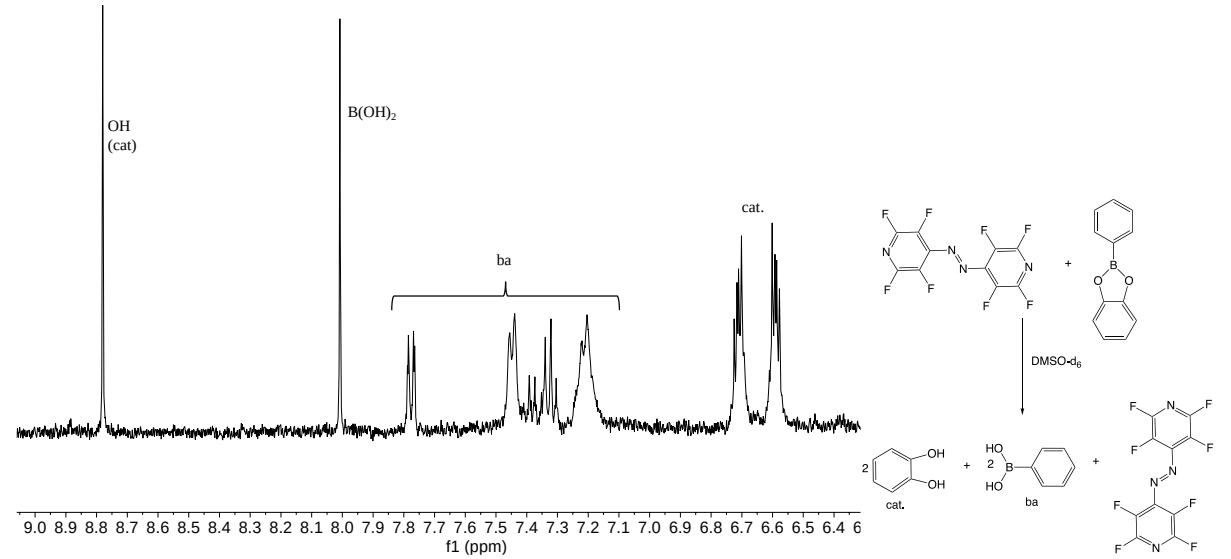

Figure S24. ^{1}H NMR spectra of (**PhBE**)·(**perF-azop**) (400 MHz, DMSO-d_6). We note the adduct dissociated in solution.

S5. Hirshfeld analysis

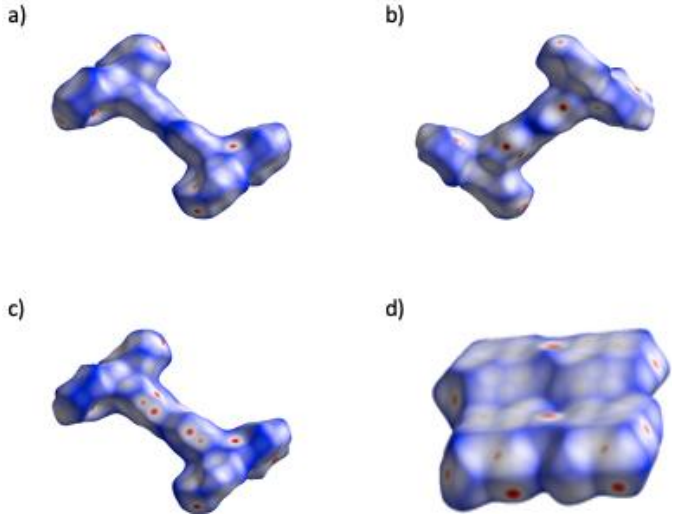

Figure S25. 2D Hirshfeld projections along the *a*-axis of adducts and co-crystal: a) (**PhBE**)·(**azop**), b) (**PhBE**)·(**diF-azop**), c) (**PhBE**)·(**tetraF-azop**), and d) (**PhBE**)·(**perF-azop**).

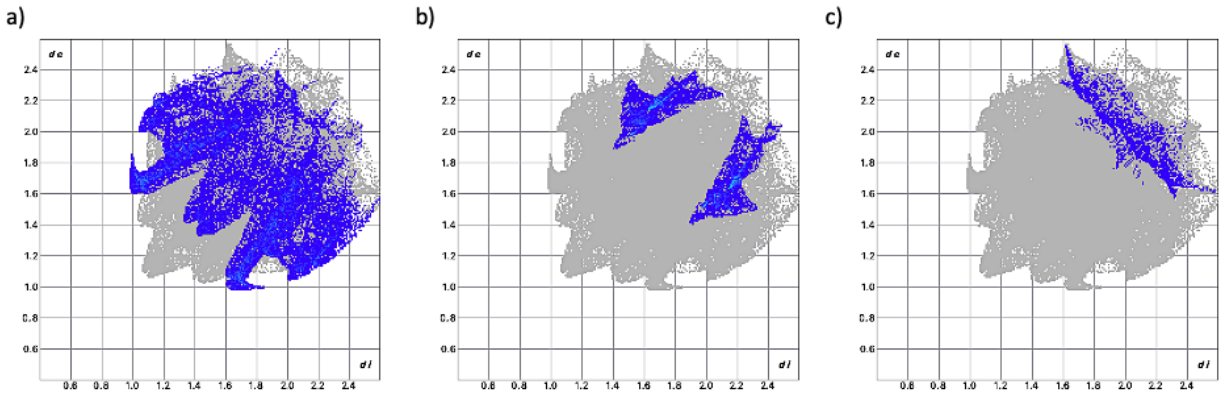

Figure S26. Selected Hirshfeld projection interactions for (**PhBE**)·(**azop**) structure: a) C-C interactions, b) C-H interactions, and c) N-H interactions.

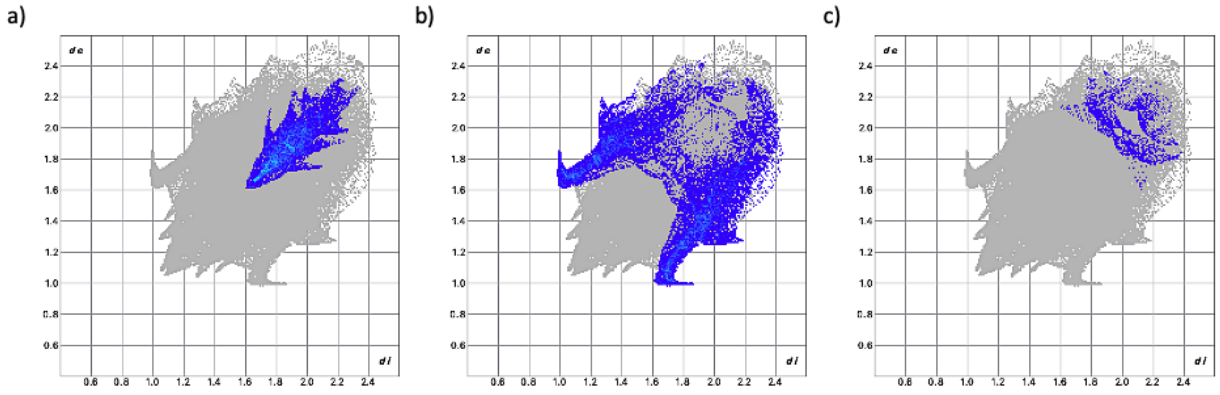

Figure S27. Selected Hirshfeld projection interactions for (**PhBE**)·(**diFazop**) structure: a) C-C interactions, b) C-H interactions, and c) N-H interactions.

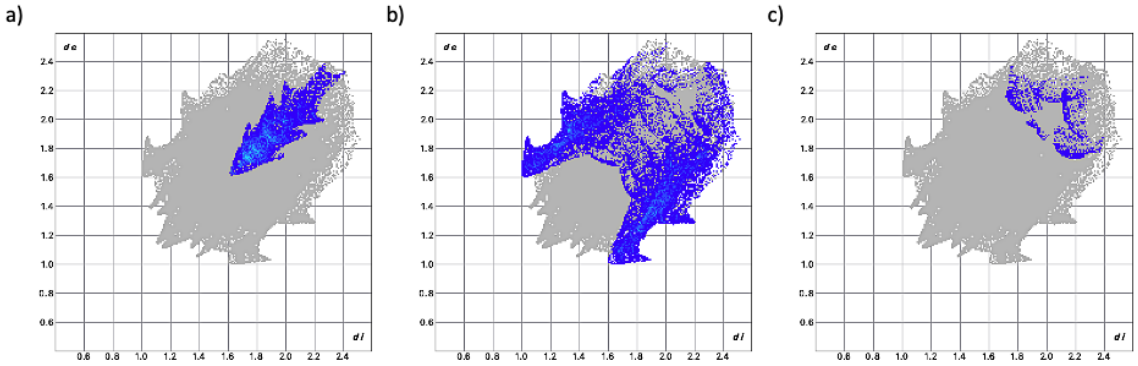

Figure S28. Selected Hirshfeld projection interactions for (**PhBE**)·(**tetraF-azop**) structure: a) C-C interactions, b) C-H interactions, and c) N-H interactions.

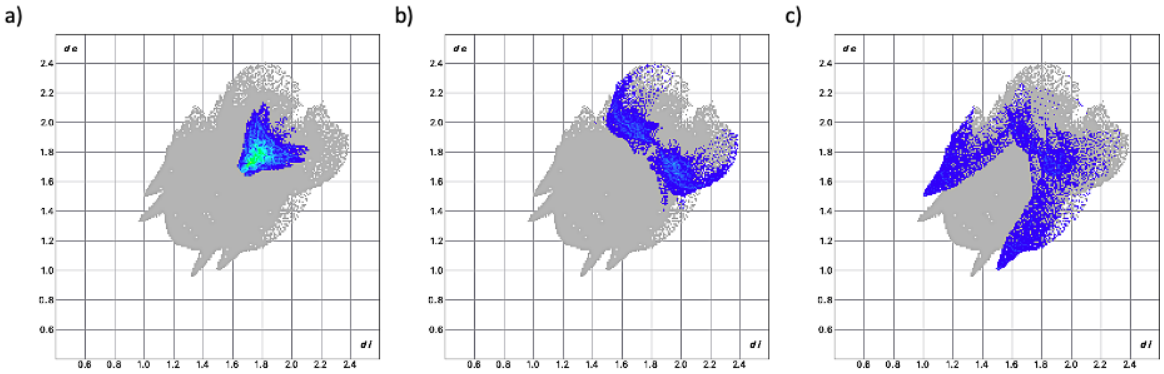

Figure S29. Selected Hirshfeld projection interactions for (**PhBE**)·(**perF-azop**) structure: a) C-C interactions, b) C-H interactions, and c) N-H interactions.

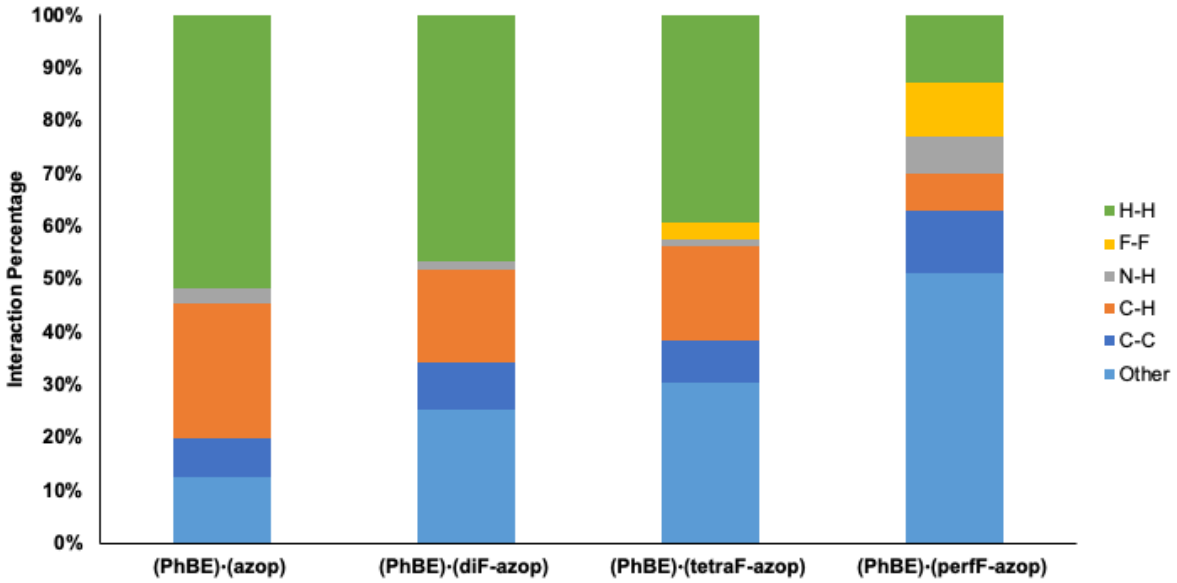

Table S8. Selected projection interaction percentages of the reported cocrystal structures.

References

1. N. Iranpoor, H. Firouzabadi, D. Khalili and S. Motevalli, *J. Org. Chem.*, 2008, **73**, 4882-4887.
2. G. M. Sheldrick, *Acta Cryst. A*, 2015, **71**, 3-8.
3. G. M. Sheldrick, *Acta Cryst. C*, 2015, **71**, 3-8.
4. O. V. Dolomanov, L. J. Bourhis, R. J. Gildea, J. A. Howard and H. Puschmann, *J. Appl. Crystallogr.*, 2009, **42**, 339-341.
5. (a) J.-D. Chai and M. Head-Gordon, *Phys. Chem. Chem. Phys.*, 2008, **10**, 6615-6620; (b) Y. K. Kang and H. S. Park, *Chem. Phys. Lett.*, 2014, **600**, 112-117.
6. H. Putz and K. Brandenburg GbR, Match! - Phase Analysis using Powder Diffraction (version Version 3) Crystal Impact, Kreuzherrenstr. 102 53227 Bonn, Germany.